

## Thermodynamic Geometry of Microscopic Heat Engines

Kay Brandner<sup>1,2</sup> and Keiji Saito<sup>2</sup>

<sup>1</sup>Department of Applied Physics, Aalto University, 00076 Aalto, Finland

<sup>2</sup>Department of Physics, Keio University, 3-14-1 Hiyoshi, Yokohama 223-8522, Japan

 (Received 19 July 2019; published 29 January 2020)

We develop a general framework to describe the thermodynamics of microscopic heat engines driven by arbitrary periodic temperature variations and modulations of a mechanical control parameter. Within the slow-driving regime, our approach leads to a universal trade-off relation between efficiency and power, which follows solely from geometric arguments and holds for any thermodynamically consistent microdynamics. Focusing on Lindblad dynamics, we derive a second bound showing that coherence as a genuine quantum effect inevitably reduces the performance of slow engine cycles regardless of the driving amplitudes. To show how our theory can be applied in practice, we work out a specific example, which lies within the range of current solid-state technologies.

DOI: 10.1103/PhysRevLett.124.040602

The laws of thermodynamics limit the performance of thermal machines across all length and energy scales. A prime example is the Carnot bound on efficiency, which applies to James Watt's steam engine and recent small-scale engines using colloidal particles [1–3], single atoms [4,5] or engineered quantum systems [6,7] alike. Still, this bound is mostly of theoretical value as it is typically attained only by infinitely slow cycles producing zero power. Practical devices operating in finite time, however, are inevitably subject to frictional losses suppressing their efficiency. Hence, we are prompted to ask, How much performance has to be sacrificed for finite speed?

This question, which inspired the development of finite-time thermodynamics in the 1970s and 1980s [8–11], is now attracting renewed interest. Triggered by the observation that Carnot efficiency at finite power might indeed be possible in systems with broken time-reversal symmetry [12], recent studies discovered quantitative trade-off relations that rule out this option for generic heat engines [13–20]; overcoming these bounds requires exceptional conditions like diverging power fluctuations [21–23] or fine-tuned dissipation mechanisms leading to vanishing relaxation times [24–27].

These results rely on stochastic models to describe the internal dynamics of small-scale engines. Here, we pursue an alternative strategy that builds on the framework of thermodynamic geometry [28]. This approach replaces the traditional thermodynamic picture, which mixes control and response variables, with a geometric picture. The properties of the working system are thereby encoded in a vector potential and a Riemannian metric in the space of control parameters, see Fig. 1. The driving protocols define a closed path in this space and can thus be assigned an effective flux and length. In adiabatic response, these quantities provide measures for the two key figures of

merit: the work output and the minimal dissipation of the underlying thermodynamic process.

The idea of using geometric concepts to describe the thermodynamics of finite-time operations was originally conceived for macroscopic systems and developed mainly

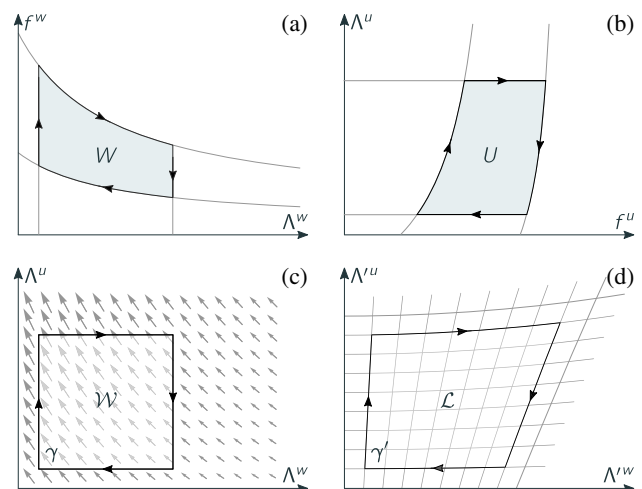


FIG. 1. Four faces of a microscopic engine cycle. Upper panel: Thermodynamic picture. The two sketches show effective pressure-volume (a) and temperature-entropy (b) diagrams for a Stirling cycle consisting of two *isochoric* ( $\Lambda^w = V = \text{const}$ ) and two *isothermal* ( $\Lambda^u = T = \text{const}$ ) strokes. The enclosed areas correspond to the generated work  $W$  and the effective input  $U$ . Lower panel: Geometric picture. In the space of control parameters  $\Lambda^u$  and  $\Lambda^w$ , the quasistatic work  $\mathcal{W}$  is given by the line integral of the thermodynamic vector potential along  $\gamma$ , i.e., the flux of the corresponding effective magnetic field through the area enclosed by this path (c). In the curvilinear coordinates  $\Lambda^w$  and  $\Lambda^u$ , which carry the thermodynamic metric,  $\gamma$  is distorted into the contour  $\gamma'$ , whose length  $\mathcal{L}$  provides a lower bound on the dissipated energy (d).

on the basis of phenomenological principles [11,28,29]. Over the last decades, this approach has been formulated on microscopic grounds [30], linked to information-theoretic quantities [28] and extended to classical nanoscale systems [31], closed quantum systems far from equilibrium [32] and, most recently, open quantum systems [33,34]. Thermodynamic geometry has thus become a powerful tool, which, as its key application, provides an elegant way to determine optimal control protocols minimizing the dissipation of isothermal processes [35–39]. Yet, this framework has neither been applied to bound the finite-time efficiency of general microscopic engine cycles nor to explore the impact of coherence on this figure.

In macroscopic thermodynamics, heat engines are described as machines that generate usable work while operating between two reservoirs, a hot one providing energy input and a cold one acting as a sink of entropy [40]. Microscopic heat engines, however, are typically driven by externally controlled heat sources [1–7]. This design enables unconventional cycles with continuous temperature profiles, which offer more freedom for optimization but cannot be described within the two-reservoir scheme.

For a more general model for small-scale engines, we consider a working system with tunable Hamiltonian  $H_V$  that is embedded in an environment with adjustable temperature  $T$ . The device is operated by cyclic variations of  $T$  and the mechanical parameter  $V$  driving the system into a periodic state  $\rho_i$ ; the vector  $\Lambda \equiv (T, V) \equiv (\Lambda^u, \Lambda^w)$  thereby passes through a closed path  $\gamma: \Lambda \mapsto \Lambda_t$ . Output and input of this process can be identified as

$$\begin{aligned} W &= \oint_{\gamma} p dV = \int_0^{\tau} dt f_t^w \dot{\Lambda}_t^w, \\ U &= \oint_{\gamma} T dS = - \int_0^{\tau} dt f_t^u \dot{\Lambda}_t^u, \end{aligned} \quad (1)$$

where  $\tau$  denotes the cycle time, dots indicate time derivatives, and the generalized forces,

$$f_t^w \equiv p_t \equiv -\text{Tr}[\rho_t \partial_V H_{V_t}], \quad f_t^u \equiv S_t \equiv -\text{Tr}[\rho_t \ln \rho_t], \quad (2)$$

correspond to the effective pressure and the entropy of the medium, respectively. Thus,  $W$  is the mean generated work and  $U$  can be regarded as the uptake of thermal energy from the heat source, i.e., the amount of energy that is available for work production under a given temperature profile. As illustrated in Fig. 1 (upper panel), the quantities  $W$  and  $U$  can be determined in practice by measuring the pressure-volume and temperature-entropy diagrams of the cycle; such measurements have recently been reported for a single-atom heat engine [5].

The identification of  $U$  as the effective input provided by the heat source can be understood from the relation

$$A \equiv U - W = - \int_0^{\tau} dt f_t^u \dot{\Lambda}_t^u = \int_0^{\tau} dt T_t \Sigma_t \geq 0, \quad (3)$$

which describes the energy balance of the engine [41]. Here,  $\Sigma_t$  is the total rate of entropy production, which must be non-negative according to the second law. Hence, the *dissipated availability*  $A$  describes the average loss of energy due to finite-time driving [42]; this quantity vanishes in the quasistatic limit and reduces to the total irreversible work for conventional two-temperature cycles [43]. Note that  $\mu = w, u$  and summation over identical indices is understood throughout.

The balance relation Eq. (3) shows that the ratio

$$\varepsilon \equiv W/U \leq 1 \quad (4)$$

provides a proper measure for the ability of a microscopic heat engine to avoid dissipative losses. This figure, which we henceforth refer to as efficiency, is well defined for arbitrary control protocols leading to positive output, i.e.,  $W > 0$ , and reaches its maximum 1 whenever the engine operates reversibly. Note that the conventional thermodynamic efficiency,  $\eta \equiv Q/W$ , which depends on the gross heat absorption per cycle,  $Q$ , admits a tight universal bound only for two-temperature profiles, where  $\eta/\eta_C \leq \varepsilon$  with  $\eta_C$  being the Carnot factor [43].

Before moving on, it is instructive to apply our general framework to the quasistatic regime, where the system follows its instantaneous Gibbs state, i.e., we have

$$\rho_t = \rho_{\Lambda_t} \quad \text{with} \quad \rho_{\Lambda} \equiv \exp[-(H_V - \mathcal{F}_{\Lambda})/T] \quad (5)$$

and  $\mathcal{F}_{\Lambda}$  denoting the Helmholtz free energy. The generalized forces, Eq. (2), can then be expressed as  $f_t^{\mu} = \mathcal{F}_{\Lambda_t}^{\mu}$  with  $\mathcal{F}_{\Lambda}^{\mu} = -\partial_{\mu} \mathcal{F}_{\Lambda}$ . Inserting this relation into Eq. (3) shows that the dissipation  $A$  vanishes; the efficiency, Eq. (4), thus attains its upper bound 1. However, since the condition Eq. (5) can be met only for infinitely long cycle times, the generated power,  $P \equiv W/\tau$ , also goes to zero and the engine becomes virtually useless. Note that we focus on generic heat engines throughout, i.e., we assume that the overall relaxation time of the working system is finite.

Increasing the driving speed leads to finite power but inevitably also to dissipation reducing  $\varepsilon$ . This trade-off can be understood quantitatively in the adiabatic response regime, where the external parameters change slowly compared to the relaxation time of the system. Under this condition, the thermodynamic forces, Eq. (2), and the control rates  $\dot{\Lambda}_t$  are connected by the linear relations

$$f_t^{\mu} = \mathcal{F}_{\Lambda_t}^{\mu} + R_{\Lambda_t}^{\mu\nu} \dot{\Lambda}_t^{\nu}, \quad (6)$$

where  $\nu = w, u$  and the adiabatic response coefficients  $R_{\Lambda_t}^{\mu\nu}$  depend parametrically on the driving protocols  $\Lambda_t$  [44]. The average energy loss [Eq. (3)] thus becomes

$$A = \int_0^\tau dt g_{\Lambda_t}^{\mu\nu} \dot{\Lambda}_t^\mu \dot{\Lambda}_t^\nu \quad \text{with} \quad g_{\Lambda}^{\mu\nu} \equiv -(R_{\Lambda}^{\mu\nu} + R_{\Lambda}^{\nu\mu})/2 \quad (7)$$

denoting the elements of a, possibly degenerate, metric tensor in the space of control parameters [45]. Thus, the Cauchy-Schwarz inequality implies

$$A \geq \mathcal{L}^2/\tau, \quad \text{where} \quad \mathcal{L} \equiv \oint_{\gamma} \sqrt{g_{\Lambda}^{\mu\nu} d\Lambda^\mu d\Lambda^\nu} \quad (8)$$

corresponds to the thermodynamic length of the path  $\gamma$ .

Expanding the efficiency [Eq. (4)] to second order in the driving rates  $\dot{\Lambda}_t$  yields  $\varepsilon = 1 - A/\mathcal{W}$ , where the quasistatic work can be expressed as a line integral,

$$\mathcal{W} \equiv - \int_0^\tau dt \mathcal{F}_{\Lambda_t}^w \dot{\Lambda}_t^w = - \oint_{\gamma} \mathcal{A}_{\Lambda}^\mu d\Lambda^\mu$$

$$\text{with} \quad \mathcal{A}_{\Lambda}^\mu \equiv \partial_\mu \mathcal{F}_{\Lambda}^w$$

being the thermodynamic vector potential. Using Eq. (8) thus yields the power-efficiency trade-off relation

$$(1 - \varepsilon)(\mathcal{W}/\mathcal{L})^2 \geq \mathcal{W}/\tau = P. \quad (9)$$

This bound implies that the power of any heat engine covered by our general model must vanish at least linearly as its efficiency approaches the ideal value 1; for two-temperature cycles, this conclusion also holds for the normalized conventional efficiency,  $\eta/\eta_C \leq \varepsilon$ . The maximal slope of this decay is determined by the thermodynamic mean force  $\mathcal{W}/\mathcal{L}$ , where  $\mathcal{L}$  and  $\mathcal{W}$  are geometric quantities, i.e., they are independent of the parameterization of the control path  $\gamma$ , see Fig. 1 (lower panel).

Moreover, Eq. (9) entails a universal optimization principle, which arises from the observation that the bound, Eq. (8), becomes an equality if the path  $\gamma$  is parameterized in terms of its thermodynamic length. To this end,  $t$  has to be replaced with the speed function  $\phi_t$ , which is implicitly defined through the relation

$$t = \tau \int_0^{\phi_t} ds \sqrt{g_{\Lambda_s}^{\mu\nu} \dot{\Lambda}_s^\mu \dot{\Lambda}_s^\nu} / \mathcal{L}. \quad (10)$$

Thus, since  $\mathcal{W}$  is not affected by this transformation, the bound [Eq. (9)] can be saturated for any given path  $\gamma$ , whereby the efficiency [Eq. (4)] attains its geometric maximum

$$\varepsilon^* = 1 - \mathcal{L}^2/\mathcal{W}\tau. \quad (11)$$

Note that, in contrast to the common strategy of optimizing the mechanical protocol for a given temperature profile [46–52], this scheme exploits the freedom of external control over the working temperature of the engine.

Holding for any thermodynamically consistent microdynamics, our general analysis so far applies to classical and quantum heat engines alike. To explore the fundamental differences between these two regimes, we now model the time evolution of the working medium explicitly using the well-established adiabatic Lindblad approach. This scheme rests on the assumption that the modulations of the system Hamiltonian and the rate at which the external heat source provides thermal energy are both slow compared to the relaxation time of the environment and the unitary evolution of the bare medium. Applying this condition together with the standard weak-coupling approximation and a coarse graining in time to wipe out memory effects and fast oscillations yields the Markovian master equation

$$\begin{aligned} \partial_t \rho_t &= \mathcal{L}_{\Lambda} \rho_t \quad \text{with} \\ \mathcal{L}_{\Lambda} X &\equiv -\frac{i}{\hbar} [H_V, X] + \sum_{\sigma} ([J_{\Lambda}^{\sigma} X, J_{\Lambda}^{\sigma\dagger}] + [J_{\Lambda}^{\sigma}, X J_{\Lambda}^{\sigma\dagger}]). \end{aligned} \quad (12)$$

Here,  $\hbar$  denotes Planck's constant and the Lindblad generator  $\mathcal{L}_{\Lambda}$  depends parametrically on the driving protocols  $\Lambda_t$ , for details see Ref. [53] and Refs. [18,54–59]. Using Eq. (12), the periodic state  $\rho_t$  can be determined by means of an adiabatic perturbation theory [60,61].

This procedure, which we outline in Ref. [53], yields the Green-Kubo type expression

$$R_{\Lambda}^{\mu\nu} = -\frac{1}{T} \int_0^\infty dt \langle\langle \exp[\mathcal{K}_{\Lambda} t] F_{\Lambda}^{\mu} | F_{\Lambda}^{\nu} \rangle\rangle \quad (13)$$

for the adiabatic response coefficients, where the canonical correlation function is defined as

$$\langle\langle X|Y \rangle\rangle \equiv \int_0^1 dx \text{Tr}[e_{\Lambda}^{1-x} X e_{\Lambda}^x Y] - \text{Tr}[e_{\Lambda} X] \text{Tr}[e_{\Lambda} Y] \quad (14)$$

for arbitrary observables  $X$  and  $Y$ ;  $\rho_{\Lambda}$  denotes the Gibbs state defined in Eq. (5), the force operators are given by

$$F_{\Lambda}^w \equiv -\partial_V H_V \quad \text{and} \quad F_{\Lambda}^u \equiv -\ln e_{\Lambda} \quad (15)$$

and the adjoint Lindblad generator  $\mathcal{K}_{\Lambda}$  is defined by the relation  $\text{Tr}[X \mathcal{K}_{\Lambda} Y] \equiv \text{Tr}[Y \mathcal{L}_{\Lambda} X]$  [62]. This super operator is subject to three general consistency requirements. First, since we now work on a coarse-grained time scale, where coherent oscillations have been averaged out, the operators  $J_{\Lambda}^{\sigma}$  can only induce jumps between the energy levels of the working system [58]. Hence, the eigenstates of  $H_V$  form the preferred basis of the dynamics and  $\mathcal{K}_{\Lambda}$  obeys the invariance condition

$$\mathcal{K}_{\Lambda}[H_V, X] = [H_V, \mathcal{K}_{\Lambda} X]. \quad (16)$$

Second, owing to microreversibility, the generators  $\mathcal{K}_{\Lambda}$  and  $\mathcal{L}_{\Lambda}$  are connected by symmetry relation [18]

$$\mathbb{T}e_{\Lambda}K_{\Lambda}X = L_{\Lambda}e_{\Lambda}TX, \quad (17) \quad \varepsilon^* \leq 1 - (\mathcal{L}_d^2 + \mathcal{L}_c^2)/\mathcal{W}\tau, \quad (21)$$

where the super operator  $\mathbb{T}$  induces time reversal [18] and we assume that no magnetic field is applied to the system, i.e.,  $\mathbb{T}H_V = H_V$  and  $\mathbb{T}J_{\Lambda}^{\sigma} = J_{\Lambda}^{\sigma}$ . Together with Eq. (16), this property implies the adiabatic reciprocity relation  $R_{\Lambda}^{\mu\nu} = R_{\Lambda}^{\nu\mu}$ , which resembles the familiar Onsager symmetry of linear irreversible thermodynamics [63,64]. Third, as a technical requirement, we understand that the jump operators  $J_{\Lambda}^{\sigma}$  form a self-adjoint and irreducible set; this condition ensures that, for  $\Lambda$  fixed, the mean of any observable relaxes to its unique equilibrium value under the dynamics generated by  $K_{\Lambda}$  in the Heisenberg picture [65]. The expression Eq. (13) is then well defined over the entire space of control parameters [66].

We are now ready to analyze the impact of quantum effects on slowly driven heat engines from a geometric perspective. To this end, we first divide the mechanical force operator into a diagonal and a coherent part,

$$F_{\Lambda}^w \equiv F_{\Lambda}^d + i[H_V, G_V] \equiv F_{\Lambda}^d + F_{\Lambda}^c. \quad (18)$$

Here,  $F_{\Lambda}^d$  commutes with  $H_V$  and  $G_V$  corresponds to an adiabatic gauge potential [61]. Upon inserting this decomposition into Eq. (13), the adiabatic response coefficients decay into two components,

$$R_{\Lambda}^{\mu\nu} = D_{\Lambda}^{\mu\nu} + \delta_{\mu\nu}\delta_{\nu w}C_{\Lambda}^{ww}, \quad (19)$$

where  $D_{\Lambda}^{\mu\nu}$  and  $C_{\Lambda}^{ww}$  are given by Eq. (13) with  $F_{\Lambda}^w$  replaced by  $F_{\Lambda}^d$  and  $F_{\Lambda}^c$ , respectively; the cross terms between  $F_{\Lambda}^c$  and the diagonal operators  $F_{\Lambda}^d$  and  $F_{\Lambda}^c$  vanish due to the property [Eq. (16)] of the adjoint generator. Next, by plugging Eq. (19) into the definition Eq. (8) of the thermodynamic length and using the concavity of the square-root function, we arrive at the bound [68]

$$\mathcal{L} \geq \sqrt{\mathcal{L}_d^2 + \mathcal{L}_c^2}. \quad (20)$$

The two quantities on the right, which are defined as

$$\mathcal{L}_d \equiv \oint_{\gamma} \sqrt{-D_{\Lambda}^{\mu\nu}d\Lambda^{\mu}d\Lambda^{\nu}} \quad \text{and} \\ \mathcal{L}_c \equiv \oint_{\gamma} \sqrt{-C_{\Lambda}^{ww}d\Lambda^w d\Lambda^w},$$

thereby describe two genuinely different types of energy losses: the reduced thermodynamic length  $\mathcal{L}_d$  accounts for the dissipation of heat in the environment and the quantum correction  $\mathcal{L}_c$  arises from the decay of superpositions between the energy levels of the working system, a mechanism known as quantum friction [69–73].

The constraint [Eq. (20)] puts an upper limit on the optimal finite-time efficiency [Eq. (11)]. This bound,

is saturated in the quasiclassical limit, where  $F_{\Lambda}^c = 0$ ; the energy eigenstates of the system are then time independent and the periodic state  $\rho_t$  is diagonal in this basis throughout the cycle. In fact, since the quasistatic work  $\mathcal{W}$  is independent of  $F_{\Lambda}^c$ , the bound [Eq. (21)] shows that injecting coherence into the working system can only reduce the maximum efficiency at given power. These coherence-induced performance losses are a universal feature of the slow-driving regime, where superpositions between different energy levels are irreversibly destroyed by the environment before their work content can be extracted through mechanical operations. While similar conclusions could so far be drawn only for specific models [69–73] and small driving amplitudes [18,74], our new bound [Eq. (21)] applies to any heat engine that is covered by Lindblad dynamics and operated in adiabatic response. Thus, it further corroborates the emerging picture that quantum effects can enhance the performance of thermal machines only far from equilibrium [74–76].

To show how our results can be applied in practice, we now consider a simple model for a solid-state heat engine that is inspired by a recent experiment [7]. The working system is a superconducting qubit with Hamiltonian

$$H_V = -\frac{\hbar\Omega}{2}(\Delta\sigma_x + \sqrt{V^2 - \Delta^2}\sigma_z). \quad (22)$$

Here,  $\sigma_x$  and  $\sigma_z$  are the usual Pauli matrices,  $\hbar\Omega$  denotes the overall energy scale, and the dimensionless parameters  $\Delta \geq 0$  and  $V \geq \Delta$  correspond to the tunneling energy and the flux-tunable level-splitting of the qubit [77,78]. The role of the environment plays a normal-metal island, whose temperature can be accurately controlled with established techniques [79] and monitored by means of sensitive electron thermometers, a technology that could soon enable calorimetric work measurements [80–85]. This reservoir can be described in terms of two jump operators,  $J_{\Lambda}^+$  and  $J_{\Lambda}^-$ , defined by the conditions

$$[H_V, J_{\Lambda}^{\pm}] = \pm\hbar\Omega V J_{\Lambda}^{\pm}, \quad \text{Tr}[J_{\Lambda}^{\pm}J_{\Lambda}^{\pm\dagger}] = \frac{\pm\Gamma\Omega V}{1 - \exp[\mp\hbar\Omega V/T]},$$

where  $\Gamma$  determines the average jump frequency.

We proceed in three steps. First, we evaluate the adiabatic response coefficients for the single-qubit engine using Eq. (13). Second, we calculate the geometric quantities entering the bounds Eqs. (9) and (21) and the optimal speed function  $\phi_t$  defined in Eq. (10). For simplicity, we thereby assume that the device is driven by harmonic temperature and energy modulations, i.e., we set

$$\Lambda_t = \{\hbar\Omega(1 + \sin^2[\pi\Omega t]), 1 + \sin^2[\pi\Omega t + \pi/4]\}. \quad (23)$$

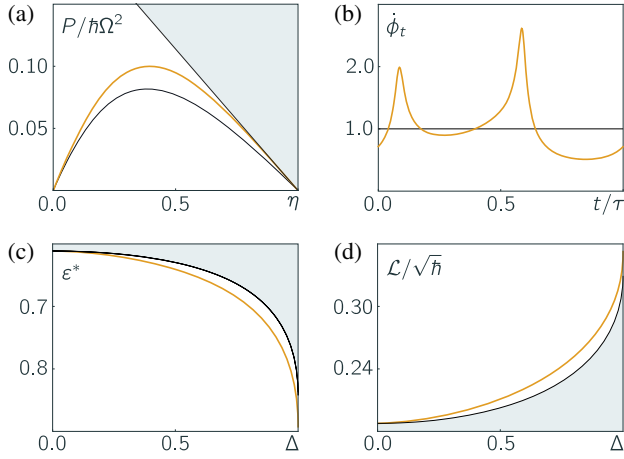


FIG. 2. Performance of a single-qubit engine. Upper panel: Geometric optimization. Plot (a) shows the relation between power and efficiency, where the cycle time is varied from  $\tau = 1/10\Omega$  to  $\tau = 50/\Omega$  at  $\Delta = 3/5$ . The two curves are obtained for linear (black) and optimal (orange) parameterization of the control path; the derivatives of the corresponding speed functions are shown in (b). The shaded area in (a) is inaccessible in adiabatic response due to our bound Eq. (9). Lower panel: Quantum losses. The orange curves show the optimal efficiency [Eq. (11)] for  $\tau = 3/\Omega$  (c) and the thermodynamic length (d) as functions of the coherence parameter  $\Delta$ ; shaded areas indicate the bounds Eqs. (21) and (20). For all plots, we set  $\Gamma = 5$ .

Hence, the control path  $\gamma$  is a circle in the  $\Lambda^u$ - $\Lambda^w$  plane. Third, in order to assess the quality of our bounds, we determine the periodic state  $\rho_t$  of the system exactly by solving the time-inhomogeneous master equation, Eq. (12), for both constant and optimal driving speed. Using the expressions Eqs. (1) and (2), the power and the efficiency of the engine can thus be obtained for any cycle time  $\tau$ .

The results of this analysis are summarized in Fig. 2, for details see Ref. [53]. We find that, for optimal driving speed, our bound Eq. (9) is practically attained in the range  $\varepsilon \gtrsim 0.8$ , which corresponds to  $\tau \gtrsim 2/\Omega$ . The optimal protocols  $\Lambda_t^* \equiv \Lambda_{\phi_t}$  thereby outperform the harmonic profiles [Eq. (23)] by roughly a factor 1.2 in power at given efficiency. Remarkably, this increase in performance persists even for  $\varepsilon < 0.8$ , i.e., for short cycle times  $\tau < 2/\Omega$ , which are not covered by the slow-driving approximation Eq. (6).

The lower panel of Fig. 2 shows that the single-qubit engine operates most efficiently in the quasiclassical configuration  $\Delta = 0$ . For this setting, the eigenstates of the Hamiltonian Eq. (22) are independent of  $V$  and our bounds Eqs. (20) and (21) are saturated. Increasing  $\Delta$  leads to more quantum friction. Hence, the thermodynamic length grows and the optimal efficiency drops, whereby both figures closely follow their upper and lower bound, respectively. This behavior underlines our general result that coherence can only reduce the efficiency of slow engine cycles. Exploring the fast-driving regime by including higher-order corrections in the expansion Eq. (6), which

could be derived with recent techniques going beyond the adiabatic master equation, Eq. (12) [59,86,87], constitutes an important problem for future investigations.

K. B. thanks P. Menczel for insightful discussions and for a careful proof reading of this manuscript and J. P. Pekola for helpful comments. K. B. acknowledges support from Academy of Finland (Contract No. 296073) and is associated with the Centre for Quantum Engineering at Aalto University. K. S. was supported by JSPS Grants-in-Aid for Scientific Research (JP17K05587, JP16H02211). K. B. performed part of this work as an International Research Fellow of the Japan Society for the Promotion of Science (Fellowship ID: P19026).

- [1] V. Blicke and C. Bechinger, Realization of a micrometer-sized stochastic heat engine, *Nat. Phys.* **8**, 143 (2012).
- [2] I. A. Martínez, É. Roldán, L. Dinis, D. Petrov, J. M. R. Parrondo, and R. A. Rica, Brownian Carnot engine, *Nat. Phys.* **12**, 67 (2016).
- [3] I. A. Martínez, É. Roldán, L. Dinis, D. Petrov, and R. A. Rica, Adiabatic Processes Realized with a Trapped Brownian Particle, *Phys. Rev. Lett.* **114**, 120601 (2015).
- [4] O. Abah, J. Roßnagel, G. Jacob, S. Deffner, F. Schmidt-Kaler, K. Singer, and E. Lutz, Single-Ion Heat Engine at Maximum Power, *Phys. Rev. Lett.* **109**, 203006 (2012).
- [5] J. Roßnagel, S. T. Dawkins, K. N. Tolazzi, O. Abah, E. Lutz, F. Schmidt-Kaler, and K. Singer, A single-atom heat engine, *Science* **352**, 325 (2016).
- [6] J. Klatzow, J. N. Becker, P. M. Ledingham, C. Weinzettl, K. T. Kaczmarek, D. J. Saunders, J. Nunn, I. A. Walmsley, R. Uzdin, and E. Poem, Experimental Demonstration of Quantum Effects in the Operation of Microscopic Heat Engines, *Phys. Rev. Lett.* **122**, 110601 (2019).
- [7] A. Ronzani, B. Karimi, J. Senior, Y.-C. Chang, J. T. Peltonen, C. D. Chen, and J. P. Pekola, Tunable photonic heat transport in a quantum heat valve, *Nat. Phys.* **14**, 911 (2018).
- [8] F. Weinhold, Metric geometry of equilibrium thermodynamics, *J. Chem. Phys.* **63**, 2479 (1975).
- [9] R. Gilmore, Length, and curvature in the geometry of thermodynamics, *Phys. Rev. A* **30**, 1994 (1984).
- [10] B. Andresen, R. S. Berry, R. Gilmore, E. Ihrig, and P. Salamon, Thermodynamic geometry and the metrics of Weinhold and Gilmore, *Phys. Rev. A* **37**, 845 (1988).
- [11] B. Andresen, Current trends in finite-time thermodynamics, *Angew. Chem. Int. Ed.* **50**, 2690 (2011).
- [12] G. Benenti, K. Saito, and G. Casati, Thermodynamic Bounds on Efficiency for Systems with Broken Time-Reversal Symmetry, *Phys. Rev. Lett.* **106**, 230602 (2011).
- [13] K. Brandner, K. Saito, and U. Seifert, Strong Bounds on Onsager Coefficients and Efficiency for Three-Terminal Thermoelectric Transport in a Magnetic Field, *Phys. Rev. Lett.* **110**, 070603 (2013).
- [14] K. Brandner, K. Saito, and U. Seifert, Thermodynamics of Micro- and Nano-Systems Driven by Periodic Temperature Variations, *Phys. Rev. X* **5**, 031019 (2015).

- [15] K. Brandner and U. Seifert, Bound on thermoelectric power in a magnetic field within linear response, *Phys. Rev. E* **91**, 012121 (2015).
- [16] K. Proesmans and C. Van den Broeck, Onsager Coefficients in Periodically Driven Systems, *Phys. Rev. Lett.* **115**, 090601 (2015).
- [17] K. Proesmans, B. Cleuren, and C. Van den Broeck, Power-Efficiency-Dissipation Relations in Linear Thermodynamics, *Phys. Rev. Lett.* **116**, 220601 (2016).
- [18] K. Brandner and U. Seifert, Periodic thermodynamics of open quantum systems, *Phys. Rev. E* **93**, 062134 (2016).
- [19] N. Shiraishi, K. Saito, and H. Tasaki, Universal Trade-Off Relation between Power and Efficiency for Heat Engines, *Phys. Rev. Lett.* **117**, 190601 (2016).
- [20] N. Shiraishi and K. Saito, Fundamental relation between entropy production and heat current, *J. Stat. Phys.* **174**, 433 (2019).
- [21] M. Campisi and R. Fazio, The power of a critical heat engine, *Nat. Commun.* **7**, 11895 (2016).
- [22] P. Pietzonka and U. Seifert, Universal Trade-Off between Power, Efficiency, and Constancy in Steady-State Heat Engines, *Phys. Rev. Lett.* **120**, 190602 (2018).
- [23] V. Holubec and A. Ryabov, Work and power fluctuations in a critical heat engine, *Phys. Rev. E* **96**, 030102(R) (2017).
- [24] A. E. Allahverdyan, K. V. Hovhannisyan, A. V. Melkikh, and S. G. Gevorkian, Carnot Cycle at Finite Power: Attainability of Maximal Efficiency, *Phys. Rev. Lett.* **111**, 050601 (2013).
- [25] M. Poletini and M. Esposito, Carnot efficiency at divergent power output, *Europhys. Lett.* **118**, 40003 (2017).
- [26] V. Holubec and A. Ryabov, Diverging, but negligible power at Carnot efficiency: Theory and experiment, *Phys. Rev. E* **96**, 062107 (2017).
- [27] V. Holubec and A. Ryabov, Cycling Tames Power Fluctuations Near Optimum Efficiency, *Phys. Rev. Lett.* **121**, 120601 (2018).
- [28] G. Ruppeiner, Riemannian geometry in thermodynamic fluctuation theory, *Rev. Mod. Phys.* **67**, 605 (1995).
- [29] B. Andresen, P. Salamon, and R. S. Berry, Thermodynamics in finite time, *Phys. Today* **37**, No. 9, 62 (1984).
- [30] D. Brody and N. Rivier, Geometrical aspects of statistical mechanics, *Phys. Rev. E* **51**, 1006 (1995).
- [31] G. E. Crooks, Measuring Thermodynamic Length, *Phys. Rev. Lett.* **99**, 100602 (2007).
- [32] S. Deffner and E. Lutz, Thermodynamic length for far-from-equilibrium quantum systems, *Phys. Rev. E* **87**, 022143 (2013).
- [33] M. Scandi and M. Perarnau-Llobet, Thermodynamic length in open quantum systems, *Quantum* **3**, 197 (2018).
- [34] P. Abiuso and M. Perarnau-Llobet, Optimal cycles for low-dissipation heat engines, [arXiv:1907.02939](https://arxiv.org/abs/1907.02939).
- [35] P. R. Zulkowski, D. A. Sivak, G. E. Crooks, and M. R. DeWeese, Geometry of thermodynamic control, *Phys. Rev. E* **86**, 041148 (2012).
- [36] D. A. Sivak and G. E. Crooks, Thermodynamic Metrics and Optimal Paths, *Phys. Rev. Lett.* **108**, 190602 (2012).
- [37] G. M. Rotskoff and G. E. Crooks, Optimal control in non-equilibrium systems: Dynamic Riemannian geometry of the Ising model, *Phys. Rev. E* **92**, 060102(R) (2015).
- [38] B. B. Machta, Dissipation Bound for Thermodynamic Control, *Phys. Rev. Lett.* **115**, 260603 (2015).
- [39] H. J. D. Miller, M. Scandi, J. Anders, and M. Perarnau-Llobet, Work Fluctuations in Slow Processes: Quantum Signatures and Optimal Control, *Phys. Rev. Lett.* **123**, 230603 (2019).
- [40] H. B. Callen, *Thermodynamics and an Introduction to Thermostatistics*, 2nd ed. (John Wiley & Sons, New York, 1985).
- [41] To derive Eq. (3), recall Eq. (1) and apply the first law,  $\dot{E}_t = J_t - P_t$ , to find  $-f_t^w \dot{\Lambda}_t^w - f_t^u \dot{\Lambda}_t^u = T_t \Sigma_t + \partial_t(E_t - T_t S_t)$ , where  $\Sigma_t \equiv \dot{S}_t - J_t/T_t \geq 0$  corresponds to the total rate of entropy production. Here,  $E_t$  and  $S_t = f_t^u$  denote the internal energy and entropy of the system, respectively,  $J_t$  is the rate of heat uptake from the environment and  $P_t$  the instantaneous power.
- [42] P. Salamon and R. S. Berry, Thermodynamic Length and Dissipated Availability, *Phys. Rev. Lett.* **51**, 1127 (1983).
- [43] Specifically,  $A = U - W = (T' - T)\Delta S - W \geq Q\eta_C - W$ , where  $T$  and  $T' > T$  are the two temperature levels of the cycle,  $Q$  and  $\Delta S$  are the heat uptake and the entropy change in the working system during the hot phase, respectively,  $\eta_C \equiv 1 - T/T'$  denotes the Carnot factor and the inequality follows from the second law,  $\Delta S - Q/T' \geq 0$ . Hence, we also have  $U \geq Q\eta_C$  for two-temperature cycles.
- [44] L. D'Alessio and A. Polkovnikov, Emergent Newtonian dynamics and the geometric origin of mass, *Ann. Phys. (Amsterdam)* **345**, 141 (2014).
- [45] Note that the matrix  $g_A^{\mu\nu}$  must be positive semi-definite, since the second law requires  $A \geq 0$  for any closed path  $\gamma$  and any parameterization.
- [46] T. Schmiedl and U. Seifert, Efficiency at maximum power: An analytically solvable model for stochastic heat engines, *Europhys. Lett.* **81**, 20003 (2008).
- [47] V. Holubec, An exactly solvable model of a stochastic heat engine: Optimization of power, power fluctuations and efficiency, *J. Stat. Mech.* (2014) P05022.
- [48] A. Dechant, N. Kiesel, and E. Lutz, All-Optical Nano-mechanical Heat Engine, *Phys. Rev. Lett.* **114**, 183602 (2015).
- [49] V. Holubec and A. Ryabov, Efficiency at and near maximum power of low-dissipation heat engines, *Phys. Rev. E* **92**, 052125 (2015).
- [50] M. Bauer, K. Brandner, and U. Seifert, Optimal performance of periodically driven, stochastic heat engines under limited control, *Phys. Rev. E* **93**, 042112 (2016).
- [51] A. Dechant, N. Kiesel, and E. Lutz, Underdamped stochastic heat engine at maximum efficiency, *Europhys. Lett.* **119**, 50003 (2017).
- [52] A. P. Solon and J. M. Horowitz, Phase Transition in Protocols Minimizing Work Fluctuations, *Phys. Rev. Lett.* **120**, 180605 (2018).
- [53] See Supplemental Material at <http://link.aps.org/supplemental/10.1103/PhysRevLett.124.040602> for further details on the adiabatic Lindblad approach and worked out calculations for the single-qubit heat engine.
- [54] R. Alicki, The quantum open system as a model of the heat engine, *J. Phys. A* **12**, L103 (1979).

- [55] E. Geva and R. Kosloff, Three-level quantum amplifier as a heat engine: A study in finite-time thermodynamics, *Phys. Rev. E* **49**, 3903 (1994).
- [56] D. A. Lidar, Z. Bihary, and K. B. Whaley, From completely positive maps to the quantum Markovian semigroup master equation, *Chem. Phys.* **268**, 35 (2001).
- [57] T. Albash, S. Boixo, D. A. Lidar, and P. Zanardi, Quantum adiabatic Markovian master equations, *New J. Phys.* **14**, 123016 (2012).
- [58] C. Majenz, T. Albash, H.-P. Breuer, and D. A. Lidar, Coarse graining can beat the rotating-wave approximation in quantum Markovian master equations, *Phys. Rev. A* **88**, 012103 (2013).
- [59] R. Dann, A. Levy, and R. Kosloff, Time-dependent Markovian quantum master equation, *Phys. Rev. A* **98**, 052129 (2018).
- [60] V. Cavina, A. Mari, and V. Giovannetti, Slow Dynamics and Thermodynamics of Open Quantum Systems, *Phys. Rev. Lett.* **119**, 050601 (2017).
- [61] P. Weinberg, M. Bukov, L. D'Alessio, A. Polkovnikov, S. Vajna, and M. Kolodrubetz, Adiabatic perturbation theory and geometry of periodically-driven systems, *Phys. Rep.* **688**, 1 (2017).
- [62] Specifically, the adjoint Lindblad generator is given by  $K_{\Lambda}X \equiv (i/\hbar)[H_V, X] + \sum_{\sigma} (J_{\Lambda}^{\sigma\dagger}[X, J_{\Lambda}^{\sigma}] + [J_{\Lambda}^{\sigma\dagger}, X]J_{\Lambda}^{\sigma})$ .
- [63] L. Onsager, Reciprocal relations in irreversible processes I, *Phys. Rev.* **37**, 405 (1931).
- [64] L. Onsager, Reciprocal relations in irreversible processes II, *Phys. Rev.* **38**, 2265 (1931).
- [65] H. Spohn, An algebraic condition for the approach to equilibrium of an open N-level system, *Lett. Math. Phys.* **2**, 33 (1977).
- [66] More generally, the third condition ensures that any solution of the master equation (12) converges to a unique periodic state for arbitrary cyclic protocols  $\Lambda_t$  [67].
- [67] P. Menczel and K. Brandner, Limit cycles in periodically driven open quantum systems, *J. Phys. A* **52**, 43LT01 (2019).
- [68] To derive (20), observe that  $\mathcal{L} \geq \sqrt{\alpha}\mathcal{L}_d + \sqrt{1-\alpha}\mathcal{L}_c$  for  $0 \leq \alpha \leq 1$  by the concavity of the square root function. Maximizing the right-hand side of this inequality with respect to  $\alpha$  yields the desired result.
- [69] R. Kosloff and T. Feldmann, Discrete four-stroke quantum heat engine exploring the origin of friction, *Phys. Rev. E* **65**, 055102(R) (2002).
- [70] T. Feldmann and R. Kosloff, Quantum four-stroke heat engine: Thermodynamic observables in a model with intrinsic friction, *Phys. Rev. E* **68**, 016101 (2003).
- [71] T. Feldmann and R. Kosloff, Characteristics of the limit cycle of a reciprocating quantum heat engine, *Phys. Rev. E* **70**, 046110 (2004).
- [72] T. Feldmann and R. Kosloff, Quantum lubrication: Suppression of friction in a first-principles four-stroke heat engine, *Phys. Rev. E* **73**, 025107(R) (2006).
- [73] T. Feldmann and R. Kosloff, Short time cycles of purely quantum refrigerators, *Phys. Rev. E* **85**, 051114 (2012).
- [74] K. Brandner, M. Bauer, and U. Seifert, Universal Coherence-Induced Power Losses of Quantum Heat Engines in Linear Response, *Phys. Rev. Lett.* **119**, 170602 (2017).
- [75] R. Uzdin, A. Levy, and R. Kosloff, Equivalence of Quantum Heat Machines, and Quantum-Thermodynamic Signatures, *Phys. Rev. X* **5**, 031044 (2015).
- [76] R. Uzdin, Coherence-Induced Reversibility and Collective Operation of Quantum Heat Machines via Coherence Recycling, *Phys. Rev. Applied* **6**, 024004 (2016).
- [77] A. O. Niskanen, Y. Nakamura, and J. P. Pekola, Information entropic superconducting microcooler, *Phys. Rev. B* **76**, 174523 (2007).
- [78] B. Karimi and J. P. Pekola, Otto refrigerator based on a superconducting qubit-classical and quantum performance, *Phys. Rev. B* **94**, 184503 (2016).
- [79] F. Giazotto, T. T. Heikkilä, A. Luukanen, A. M. Savin, and J. P. Pekola, Opportunities for mesoscopies in thermometry and refrigeration: Physics and applications, *Rev. Mod. Phys.* **78**, 217 (2006).
- [80] M. Campisi, J. P. Pekola, and R. Fazio, Nonequilibrium fluctuations in quantum heat engines: Theory, example, and possible solid state experiments, *New J. Phys.* **17**, 035012 (2015).
- [81] K. L. Viisanen, S. Suomela, S. Gasparinetti, O.-P. Saira, J. Ankerhold, and J. P. Pekola, Incomplete measurement of work in a dissipative two level system, *New J. Phys.* **17**, 055014 (2015).
- [82] S. Gasparinetti, K. L. Viisanen, O.-P. Saira, T. Faivre, M. Arzeo, M. Meschke, and J. P. Pekola, Fast Electron Thermometry for Ultrasensitive Calorimetric Detection, *Phys. Rev. Applied* **3**, 014007 (2015).
- [83] A. Kupiainen, P. Muratore-Ginanneschi, J. Pekola, and K. Schwieger, Fluctuation relation for qubit calorimetry, *Phys. Rev. E* **94**, 062127 (2016).
- [84] B. Donvil, P. Muratore-Ginanneschi, J. P. Pekola, and K. Schwieger, Model for calorimetric measurements in an open quantum system, *Phys. Rev. A* **97**, 052107 (2018).
- [85] L. B. Wang, O. Saira, and J. P. Pekola, Fast thermometry with a proximity Josephson junction, *Appl. Phys. Lett.* **112**, 013105 (2018).
- [86] R. Dann and R. Kosloff, The inertial theorem, *arXiv*: 1810.12094.
- [87] R. Dann, A. Tobalina, and R. Kosloff, Shortcut to Equilibration of an Open Quantum System, *Phys. Rev. Lett.* **122**, 250402 (2019).